

A Causal Modeling Framework with Stochastic Confounders

Thanh Vinh Vo

National University of Singapore
vinhvt@comp.nus.edu.sg

Wicher Bergsma

London School of Economics
w.p.bergsma@lse.ac.uk

Pengfei Wei

National University of Singapore
dcsweip@nus.edu.sg

Tze-Yun Leong

National University of Singapore
leongty@comp.nus.edu.sg

Abstract

This work aims to extend the current causal inference framework to incorporate stochastic confounders by exploiting the Markov property. We further develop a robust and simple algorithm for accurately estimating the causal effects based on the observed outcomes, treatments, and covariates, without any parametric specification of the components and their relations. This is in contrast to the state-of-the-art approaches that involve careful parameterization of deep neural networks for causal inference. Far from being a triviality, we show that the proposed algorithm has profound significance to temporal data in both a qualitative and quantitative sense.

1 Introduction

The study of causal effects of an intervention or treatment on a specific outcome based on observational data is a fundamental problem in many applications. Examples include understanding the effects of massive wildfires on a person’s mental health, of teaching methods on a student’s employability, or of disease outbreaks on the global stock market.

A critical problem of causal inference from observational data is confounding. A variable that affects both the treatment and the outcome is known as a confounder of the treatment effects on the outcome. Standard ways to measure observable confounders include propensity score matching and their variants (Rubin, 2005). However, if a confounder is hidden, the treatment effect on the outcome cannot be directly estimated without further assumptions (Pearl, 2009; Louizos et al., 2017). For example, household income, which cannot be easily measured, can affect both the therapy options available to a patient and the health condition after therapy of that patient.

Preprint. Work in progress.

Recent studies in causal inference (Shalit et al., 2017; Louizos et al., 2017; Madras et al., 2019) mainly focus on static data; the observational data are independent and identically distributed (*iid*), and time-independent. In many real-world applications, however, the events change over time, e.g., each participant may receive an intervention multiple times and the timing of these interventions may differ across participants. In this case, the *iid* assumption does not hold, and causal inference in the models would degenerate as they fail to capture the nature of time-dependent data. In practice, one can often find temporal confounders, such as seasonality and long-term trends, which can partially contribute to confounding bias.

We characterize the latent confounding effects over time in causal inference from the structural causal model (SCM) (Pearl, 2000). Specifically, we model the confounder as a stochastic process. This is important as it allows us to model confounders that have intricate patterns of interdependencies and correlations over time.

Many existing causal inference methods (e.g., Louizos et al., 2017; Shalit et al., 2017; Madras et al., 2019) exploit recent developments of deep neural networks. While effective, the performance of a neural network depends on many factors such as its structure (e.g., number of layers, number of nodes, activation function) or the optimization algorithm. Tuning a neural network is challenging; different conclusions may be drawn from different network settings. We further discuss these limitations in Section 5. In this work, we propose a nonparametric variational method to estimate the causal effects of interest. Our main contributions are summarized as follows:

- We introduce a temporal causal framework with a confounder process that captures the interdependencies of unobserved confounders. This relaxes the independence assumption in recent work (e.g., Louizos et al., 2017; Madras et al., 2019). Under this setting, we introduce the concepts of causal path effects and intervention effects, and derive an approximation to measure these quantities.
- Our framework is robust and simple for accurately learning the relevant causal effects: given a time series, learning causal effects quantifies how an outcome is expected to change if we vary the treatment level or intensity. Our algorithm requires no information about how these variables are parametrically related. This is in contrast to the need of parameterizing through constructing a neural network architecture.
- We develop a nonparametric variational estimator by exploiting the kernel trick in our temporal causal framework. This estimator has a major advantage: Complex non-linear functions can be used to modulate the SCM with estimated parameters that turn out to have *closed-form* solutions. Experimental results show that the proposed estimator can effectively handle temporal data.

2 Background and related work

2.1 Structural causal models

An SCM consists of a *triplet*: exogenous variables, endogenous variables, and structural equations. The relationships among variables are represented by a directed graph where the *vertices* represent the variables and the *edges* represent their causations. Figure 1 (a), shows a causal graph with endogenous variables Y, Z, W . Here Y is the outcome variable, W is the intervention variable, and

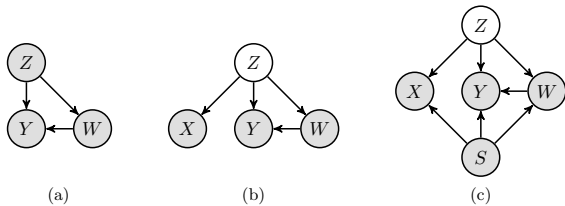


Figure 1: The SCM framework: approaches of modeling causality. (a) all variables are observed; (b) the confounder Z is latent, so it is inferred using proxy variable X (Louizos et al., 2017); (c) there is an additional observed confounder S (Madras et al., 2019).

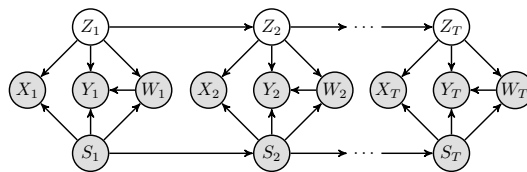


Figure 2: A causal model with stochastic confounders for temporal data.

Z is the confounder variable. Exogenous variables are variables that are not affected by any other variables in the model, which are not explicitly in the graph. Causal inference evaluates the effects of an intervention on the outcome, i.e., $p(Y | \text{do}(W))$, the distribution of the outcome Y after setting W to a specific value. The following efforts also take into account the unobserved confounders: Louizos et al. (2017); Madras et al. (2019); Montgomery et al. (2000); Riegg (2008). Specifically, some proxy variables are introduced to infer the latent confounders. For example, the household income of students is a confounder that affect the ability to afford private tuition and hence the academic performance; it may be difficult to obtain income information directly, and proxy variables such as zip code, or education level are used instead. Figure 1 (b) and (c) present two causal graphs used by the recent causal inference algorithms in Louizos et al. (2017); Madras et al. (2019). The graphs contain latent confounder Z , proxy variable X , intervention W , outcome Y , and observed confounder S .

2.2 Causal inference from temporal data

Table 1: Properties of our work compared to some recent work. Note that we only list some relevant work whose aim is to estimate causal effects.

Method	Neural Nets-Based	Representer Theorem	Potential outcomes-based	SCM-based	Latent Confounder	i.i.d Assumption	Markovian Confounder	Temporal Data
Bojinov and Shephard (2019)			✓					✓
Ning et al. (2019)			✓					✓
Osama et al. (2019)				✓	✓			
Shalit et al. (2017)	✓		✓			✓		
Louizos et al. (2017)	✓			✓	✓	✓		
Madras et al. (2019)	✓			✓	✓	✓		
Our work	✓	✓		✓	✓		✓	✓

Causal inference in existing SCM frameworks (e.g., Louizos et al., 2017; Madras et al., 2019; Pearl, 2010; Riegg, 2008) mainly handle static, *iid* data. Little attention has been paid to learning causal effects from non-*iid* data (Guo et al., 2018). Bojinov and Shephard (2019) generalized the potential outcomes framework to temporal data and developed an inference method, Horvitz–Thompson estimator (Horvitz and Thompson, 1952). Rakesh et al. (2018); Guo et al. (2018); Ning et al. (2019); Huang et al. (2019) proposed causal estimates for temporal data and developed Bayesian flavors inference methods by drawing samples of its underlying parameters from the posterior distributions. Peters et al. (2013) proposed an SCM-based model with latent confounders where the objective is to recover connections of two time series. Huang et al. (2019) proposed an autoregressive-based model which also aims to discover the connections of time series. Several efforts (e.g., Bahadori and Liu, 2012; Eichler, 2009, 2005, 2007; Eichler and Didelez, 2010; Kamiński et al., 2001) analysed causation for temporal data based on the notion of Granger causality (Granger, 1980). A summary of the properties of recent works is presented in Table 1.

Our work, in contrast, focus on evaluating the causal effects of one time series to another. Three closely related approaches are Louizos et al. (2017); Madras et al. (2019) and Shalit et al. (2017); these methods are based on variational autoencoders (VAE) and neural networks to draw inferences on causal effects. The structure of neural network, e.g., the number of layers, the activation functions, the number of nodes, etc., and the optimization method, highly affect the inference performance.

3 Our approach

3.1 Our model

We present a temporal causal framework based on SCM, as illustrated in Figure 2. We evaluate the causal effects within a *time interval* denoted by t , i.e., within the panel data setting as proposed by Frees et al. (2004). We assume that the interval is large enough to cover the effects of the treatment on the outcome.

3.1.1 The latent confounder: Z

In real world applications, capturing all the potential confounder variables is not feasible, hence some important confounder variables might not be observed. When unobserved or latent confounder variables exist, causal inference from observational data is even more challenging and, as discussed earlier, can result in biased estimation. The increasing availability of large and rich datasets, however, enables proxy variables for unobserved confounders to be inferred from other observed and correlated variables.

In practice, the exact nature and structure of the hidden or latent confounder Z are unknown. We assume that the latent confounder at time interval t , as Z_t , is normally distributed with the following Markovian property:

$$p(Z_t | \cdot) = \mathcal{N}(Z_t | f_z(Z_{t-1}), \sigma_z^2 \mathbf{I}_{D_z}), \quad (1)$$

where f_z is a function parameterizing the designated distribution, σ_z is a fixed quantity and \mathbf{I}_{D_z} denotes the identity matrix. The choice of this distribution is reasonable because each dimension of Z_t maps to a real value which gives a wide range of possible values for Z_t . Furthermore, the Gaussian assumption makes it computational tractable for subsequent calculations.

3.1.2 The observed variables: X , W , Y and S

The D_x -dimensional observed features or covariates at time interval t , is denoted by $X_t \in \mathbb{R}^{D_x}$. Similarly, the treatment variable at time interval t is given by W_t . Y_t and S_t denote a treatment outcome and the observed confounder at time interval t , respectively. Z_t denotes an unobserved confounder. As shown in Figure 2, X_t , Y_t and W_t depends on S_t and we postulate that the following holds:

$$p(S_t | \cdot) = \mathcal{N}(S_t | f_s(S_{t-1}), \sigma_s^2 \mathbf{I}_{D_s}), \quad p(X_t | \cdot) = \mathcal{N}(X_t | f_x(Z_t, S_t), \sigma_x^2 \mathbf{I}_{D_x}), \quad (2)$$

$$p(Y_t | \cdot) = \mathcal{N}(Y_t | f_y(Z_t, W_t, S_t), \sigma_y^2), \quad p(W_t | \cdot) = \text{Bern}(W_t | \varphi(f_w(Z_t, S_t))), \quad (3)$$

where f_s , f_x , f_y , f_w are functions parameterizing the designated distributions and $\varphi(\cdot)$ is the logistic function. Similar reasoning holds for these assumptions in that it gives computational tractability in terms of time series formulation.

3.1.3 Learnable functions

With Eqs. (1-3), we need to learn f_y , f_w , f_z , f_x , f_s . There are many ways to model these functions, e.g., using linear models or multi-layered neural networks. The criterion of selecting models for these functions relies on many problem-specific aspects such as types of data (e.g., text, images), dataset size (e.g., hundreds, thousands, or millions of data points), and data dimensionality (high- or low-dimension). We propose to model these functions through an augmented representer theorem, to be described in Section 4.

3.2 Causal quantities of interest

Temporal data capture the evolution of the characteristics over time. Based on earlier work (Louizos et al., 2017; Pearl, 2009; Madras et al., 2019), we perform causal inference from temporal data by assuming the Markovian property on confounders. The corresponding causal graph is shown earlier in Figure 2. This relaxes the *iid* assumption in Louizos et al. (2017) and Madras et al. (2019). In particular, we aim to measure the causal effects of W_t on Y_t given the covariate X_t , where X_t serves as the proxy variable to infer latent confounder Z_t . This formulation subsumes earlier approaches (Louizos et al., 2017; Pearl, 2009; Madras et al., 2019). Considering multiple time intervals, we further denote the notations for T time intervals as follows: $\mathbf{Y} = [Y_1, \dots, Y_T]^\top$, $\mathbf{W} = [W_1, \dots, W_T]^\top$, $\mathbf{S} = [S_1, \dots, S_T]^\top$, $\mathbf{X} = [X_1, \dots, X_T]^\top$, $\mathbf{Z} = [Z_1, \dots, Z_T]^\top$, $Z_0 = \emptyset$, $S_0 = \emptyset$.

We define *fixed-time* causal effects as the causal effects at a time interval t and *range-level* causal effects as the average causal effects in a time range. The time and range-level causal effects can be

estimated using Pearl’s *do*-calculus. We model the unobserved confounder processes using the latent variable Z_t , inferred for each observation (X_t, S_t, W_t, Y_t) at time interval t . The interval is assumed to be large enough to cover the effects of the treatment W_t on the outcome Y_t .

Definition 1 Let $\mathbf{W}_1 = [w_1^{[1]}, \dots, w_T^{[1]}]^\top$ and $\mathbf{W}_2 = [w_1^{[2]}, \dots, w_T^{[2]}]^\top$ be two treatment paths. The treatment effect path (or effect path) of $t \in [1, 2, \dots, T]$ is defined as follows

$$\text{EP} = \mathbb{E}[\mathbf{Y} \mid \text{do}(\mathbf{W} = \mathbf{W}_1), \mathbf{X}] - \mathbb{E}[\mathbf{Y} \mid \text{do}(\mathbf{W} = \mathbf{W}_2), \mathbf{X}]. \quad (4)$$

The effect path (EP) is a collection of causal effects at time interval $t \in [1, 2, \dots, T]$.

Definition 2 Let EP be the effect path satisfying Definition 1. Let $\text{EP}_t \in \text{EP}$ be the effect at time interval t . The average treatment effect (ATE) in $[T_1, T_2]$ is defined as follows

$$\text{ATE} = \left(\sum_{t=T_1}^{T_2} \text{EP}_t \right) / (T_2 - T_1 + 1). \quad (5)$$

The average treatment effect (ATE) quantifies the effects of a treatment path \mathbf{W}_1 over an alternative treatment path \mathbf{W}_2 . This work focuses on evaluating the causal effects with binary treatment. The key quantity in estimating the effect path and average treatment effects is $p(\mathbf{Y} \mid \text{do}(\mathbf{W}), \mathbf{X})$, which is the distribution of \mathbf{Y} given \mathbf{X} after setting variable \mathbf{W} by an intervention. Following Pearl’s back-door adjustment and invoking the properties of *d*-separation, the causal effects of \mathbf{W} to \mathbf{Y} given \mathbf{X} with respect to the causal graph in Figure 2 is as follows

$$p(\mathbf{Y} \mid \text{do}(\mathbf{W}), \mathbf{X}) = \int p(\mathbf{Y} \mid \mathbf{W}, \mathbf{Z}, \mathbf{S}) p(\mathbf{Z}, \mathbf{S} \mid \mathbf{X}) d\mathbf{S} d\mathbf{Z}. \quad (6)$$

Note that the expression in Eq. (6) does not typically have an analytical solution when the distributions $p(\mathbf{Y} \mid \mathbf{W}, \mathbf{Z}, \mathbf{S})$, $p(\mathbf{Z}, \mathbf{S} \mid \mathbf{X})$ are parameterized by complicated functions, e.g., a nonlinear function such as multi-layered neural network. Fortunately, we can approximate the expectation of \mathbf{Y} by an empirical expectation using Eq. (6). The procedure is as follows: First, we draw \mathbf{Z}, \mathbf{S} from

$$p(\mathbf{Z}, \mathbf{S} \mid \mathbf{X}) = \int p(\mathbf{Z} \mid \mathbf{X}, \mathbf{S}, \mathbf{W}, \mathbf{Y}) p(\mathbf{Y} \mid \mathbf{S}, \mathbf{X}, \mathbf{W}) p(\mathbf{W} \mid \mathbf{S}, \mathbf{X}) p(\mathbf{S} \mid \mathbf{X}) d\mathbf{Y} d\mathbf{W}. \quad (7)$$

Then, we substitute these samples of \mathbf{Z} and \mathbf{S} to $p(\mathbf{Y} \mid \mathbf{W}, \mathbf{Z}, \mathbf{S})$ to draw samples of \mathbf{Y} . Choosing some specific $p(\mathbf{Y} \mid \mathbf{W}, \mathbf{Z}, \mathbf{S})$, $p(\mathbf{Z} \mid \mathbf{X}, \mathbf{S}, \mathbf{W}, \mathbf{Y})$, $p(\mathbf{Y} \mid \mathbf{S}, \mathbf{X}, \mathbf{W})$, $p(\mathbf{W} \mid \mathbf{S}, \mathbf{X})$, and $p(\mathbf{S} \mid \mathbf{X})$, (6) and (7) can be sampled using forward sampling techniques. In the next section, we aim to approximate all these probability distributions.

4 Estimating causal effects

Estimating causal effects requires systematic sampling from the following distributions: $p(\mathbf{S} \mid \mathbf{X})$, $p(\mathbf{W} \mid \mathbf{S}, \mathbf{X})$, $p(\mathbf{Y} \mid \mathbf{S}, \mathbf{X}, \mathbf{W})$, $p(\mathbf{Z} \mid \mathbf{X}, \mathbf{S}, \mathbf{W}, \mathbf{Y})$, and $p(\mathbf{Y} \mid \mathbf{W}, \mathbf{Z}, \mathbf{S})$. This section presents approximations to these distributions.

4.1 The posterior of latent confounders

Exact inference of \mathbf{Z} is intractable for many models, such as multi-layered neural networks. Hence, we infer \mathbf{Z} using variational inference, which approximates the true posterior $p(\mathbf{Z} | \mathbf{X}, \mathbf{S}, \mathbf{W}, \mathbf{Y})$ by a parametric variational posterior $q(\mathbf{Z} | \mathbf{X}, \mathbf{S}, \mathbf{W}, \mathbf{Y})$. This approximation is obtained by minimizing Kullback-Leibler divergence (KL) $\mathbb{D}_{\text{KL}}[q(\mathbf{Z} | \mathbf{X}, \mathbf{S}, \mathbf{W}, \mathbf{Y}) \| p(\mathbf{Z} | \mathbf{X}, \mathbf{S}, \mathbf{W}, \mathbf{Y})]$, which is equivalent to maximizing the evidence lower bound (ELBO) of the marginal likelihood:

$$\mathcal{L} = \sum_{t=1}^T \left[\mathbb{E}_{\mathbf{Z}} \left[\log p(Y_t | W_t, S_t, Z_t) + \log p(S_t | S_{t-1}) + \log p(W_t | S_t, Z_t) + \log p(X_t | S_t, Z_t) \right] - \mathbb{E}_{\mathbf{Z}_{t-}} \left[\mathbb{D}_{\text{KL}}(q(Z_t | Y_t, X_t, W_t, S_t) \| p(Z_t | Z_{t-1})) \right] \right], \quad (8)$$

where $\mathbf{Z}_{t-} = \mathbf{Z} \setminus \{Z_t\}$ denotes vector \mathbf{Z} with $\{Z_t\}$ removed, the expectations are taken with respect to variational posterior $q(\mathbf{Z} | \mathbf{X}, \mathbf{S}, \mathbf{W}, \mathbf{Y})$, and each term in the ELBO depends on the assumption of its distribution family. The parameterized distributions of Y_t, W_t, Z_t, S_t are presented in Section 3. The variational posterior is given as follows:

$$q(Z_t | \cdot) = \mathcal{N}(Z_t | f_q(Y_t, X_t, W_t, S_t), \sigma_q^2 \mathbf{I}_{D_z}), \quad (9)$$

where f_q is a function parameterizing the designated distribution.

4.1.1 The ELBO and representer theorem

To make the functions f_y, f_w, f_z, f_x, f_s , and f_q general as stated in Section 3.1.3, we propose to model them using kernel methods. To do so, we develop a modification of the classical representer theorem (Kimeldorf and Wahba, 1970; Schölkopf et al., 2001) so that it can work well with the ELBO objective function. Since a representer theorem is developed on empirical risk loss function, so we first transform it to an empirical form.

Before presenting the empirical risk that help us in developing representer theorem for estimating causal effect, we first introduce some short notations. We denote $f_y^{t,l} = f_y(Z_t^l, W_t, S_t)$ where Z_t^l is the l -th sample from the variational posterior $q(\mathbf{Z} | \mathbf{X}, \mathbf{S}, \mathbf{W}, \mathbf{Y})$, i.e., $f_y^{t,l}$ is the value of function f_y evaluated at $[Z_t^l, W_t, S_t]$. We remark that under a reproducing kernel Hilbert space (RKHS), function f_y is understood as a vector whilst $f_y^{t,l}$ is a scalar quantity. Similarly, we also denote $f_w^{t,l} = f_w(Z_t^l, S_t)$, which is function f_w evaluated at $[Z_t^l, S_t]$. The notation on f_x is slightly different because X_t is a vector. Thus, we denote based on each of its dimension. Let $f_{x,d}^{t,l} = f_{x,d}(Z_t^l)$ be the evaluated mean of $X_{t,d}$ (d -th dimension of X_t), i.e., it is function $f_{x,d}$ evaluated at Z_t^l . Thus, $f_x^{t,l} = [f_{x,1}^{t,l}, \dots, f_{x,D_x}^{t,l}]^\top \in \mathbb{R}^{D_x}$ is the evaluated mean of vector X_t , where D_x is the number of dimensions of X_t . Similarly, because f_z is used to evaluate the mean of Z_t so the notation is also applied to each of its dimension, i.e., $f_z^{t,l} = [f_{z,1}^{t,l}, \dots, f_{z,D_z}^{t,l}]^\top$ with $f_{z,d} = f_{z,d}(Z_{t-1}^l)$. Finally, because f_s and f_q do not depend on Z_t , so we denote $f_s^t = [f_{s,1}^t, \dots, f_{s,D_s}^t]^\top$ with $f_{s,d}^t = f_{s,d}(S_{t-1})$, and $f_q^t = [f_{q,1}^t, \dots, f_{q,D_z}^t]^\top$ with $f_{q,d}^t = f_{q,d}(Y_t, X_t, W_t, S_t)$. Now we have all the necessary notations to present empirical risk loss function.

To formulate a regularized empirical risk, we draw L samples of \mathbf{Z} from the variational posterior using reparameterization trick: $\mathbf{Z}^l = [Z_1^l, \dots, Z_T^l]$ with $Z_t^l = f_q^t + \sigma_q \boldsymbol{\varepsilon}_t^l$ and $\boldsymbol{\varepsilon}_t^l \sim \mathcal{N}(0, \mathbf{I}_{D_z})$. By

drawing the noises $\varepsilon_t^1, \dots, \varepsilon_t^L$ at each time interval t in advance, we obtain a *complete* dataset

$$\mathcal{D} = \bigcup_{l=1}^L \bigcup_{t=1}^T \left\{ (Y_t, W_t, X_t, S_t, Z_t^l) \right\}.$$

At each time interval t , the dataset gives a tuple of the observed values Y_t, W_t, X_t, S_t , and an expression of $Z_t^l = f_q^t + \sigma_q \varepsilon_t^l$ where ε_t^l can also be considered as observed and σ_q is a hyperparameter. The empirical risk obtained from the negative ELBO is as follows:

$$\widehat{\mathcal{L}} = \frac{1}{L} \sum_{l=1}^L \sum_{t=1}^T \left[\frac{1}{2\sigma_y^2} (Y_t - f_y^{t,l})^2 + \frac{1}{2\sigma_s^2} \|S_t - f_s^t\|_2^2 - W_t \log \varphi(f_w^{t,l}) \right. \\ \left. - (1 - W_t) \log(1 - \varphi(f_w^{t,l})) + \frac{1}{2\sigma_x^2} \|X_t - f_x^{t,l}\|_2^2 + \frac{1}{2\sigma_z^2} \|f_q^t - f_z^{t,l}\|_2^2 \right]. \quad (10)$$

In the above equation, we remark that $f_x = \bigcup_{d=1}^{D_x} f_{x,d}$, $f_s = \bigcup_{d=1}^{D_s} f_{s,d}$, and $f_z = \bigcup_{d=1}^{D_z} f_{z,d}$. With the empirical loss function (10), it is ready to present the result of representer theorem. Instead of minimizing the empirical risk directly, we minimize its regularized version as stated in Lemma 1.

Lemma 1 *Let $\kappa_y, \kappa_w, \kappa_z, \kappa_x, \kappa_s, \kappa_q$ be kernels and $\mathcal{H}_y, \mathcal{H}_w, \mathcal{H}_z, \mathcal{H}_x, \mathcal{H}_s, \mathcal{H}_q$ be their associated reproducing kernel Hilbert space (RKHS). Let $\widehat{\mathcal{L}}(\bigcup_{i \in \mathcal{A}} f_i)$ with $\mathcal{A} = \{y, w, x, s, z, q\}$ be defined as in Eq. (10). Fix the dataset \mathcal{D} and consider minimizing the following objective function*

$$J = \widehat{\mathcal{L}}(\bigcup_{i \in \mathcal{A}} f_i) + \Omega_y(\|f_y\|_{\mathcal{H}_y}^2) + \Omega_w(\|f_w\|_{\mathcal{H}_w}^2) + \sum_{d=1}^{D_x} \Omega_x(\|f_{x,d}\|_{\mathcal{H}_x}^2) \\ + \sum_{d=1}^{D_s} \Omega_s(\|f_{s,d}\|_{\mathcal{H}_s}^2) + \sum_{d=1}^{D_z} \Omega_z(\|f_{z,d}\|_{\mathcal{H}_z}^2) + \sum_{d=1}^{D_q} \Omega_q(\|f_{q,d}\|_{\mathcal{H}_q}^2) \quad (11)$$

with respect to functions f_i ($i \in \mathcal{A}$), where Ω_i ($i \in \mathcal{A}$) are nondecreasing functions. Then, the minimizer of (11) has the following forms

$$f_y = \sum_{i=1}^T \sum_{l=1}^L \beta_{il}^y \kappa_y(\cdot, [W_i, S_i, Z_i^l]), \quad f_{x,d} = \sum_{i=1}^T \sum_{l=1}^L \beta_{il}^x[d] \kappa_x(\cdot, [S_i, Z_i^l]), \quad (12)$$

where $d = 1, \dots, D_x$. Similar forms are applied to $f_w, f_{s,d}, f_{z,d}, f_{q,d}$.

The proof is deferred to Appendix. With the above minimized form of each function, we need to specify a kernel function for each of them, and then minimize Eq. (11) with respect to the weights $\beta_{il}^{(\cdot)}, \beta_{il}^{(\cdot)}[d]$ and optionally hyperparameters of the kernels. Here we briefly describe the update rules to learn these parameters. The update rules are obtained by taking derivative of the objective function in Eq. (11) with respect to each parameter and equate to zero.

$$\beta_y = \left[\sum_{l=1}^L \mathbf{K}_y^l \mathbf{K}_y^l + 2\lambda_y L \sigma_y^2 \mathbf{K}_y \right]^{-1} \sum_{l=1}^L \mathbf{K}_y^l \mathbf{Y}, \\ \beta_{x,d} = \left[\sum_{l=1}^L \mathbf{K}_x^l \mathbf{K}_x^l + 2\lambda_x L \sigma_x^2 \mathbf{K}_x \right]^{-1} \sum_{l=1}^L \mathbf{K}_x^l \mathbf{X}_d,$$

$$\begin{aligned}\beta_{s,d} &= (\mathbf{K}_s + 2\lambda_s \sigma_s^2 \mathbf{I})^{-1} \mathbf{S}_d, \\ \beta_{z,d} &= \left[\sum_{l=1}^L \mathbf{K}_z^l \mathbf{K}_z^l + 2\lambda_z L \sigma_z^2 \mathbf{K}_z \right]^{-1} \sum_{l=1}^L \mathbf{K}_z^l \mathbf{K}_q \beta_{q,d},\end{aligned}$$

where $\mathbf{X}_d = [X_{1,d}, \dots, X_{T,d}]^\top \in \mathbb{R}^T$ with $X_{t,d}$ is the d -th dimension of X_t , similar notation applied to \mathbf{S}_d and \mathbf{Z}_d , vector $\beta_y = [\beta_{11}^y, \dots, \beta_{T1}^y, \dots, \beta_{TL}^y]^\top \in \mathbb{R}^{TL \times 1}$ and $\beta_{(\cdot,d)} = [\beta_{11}^{(\cdot)}[d], \dots, \beta_{T1}^{(\cdot)}[d], \dots, \beta_{TL}^{(\cdot)}[d]]^\top \in \mathbb{R}^{TL \times 1}$ are parameters to be estimated, $\mathbf{K}_y, \mathbf{K}_x, \mathbf{K}_s, \mathbf{K}_z \in \mathbb{R}^{TL \times TL}$ are kernel matrices computed from each pair of the dataset \mathcal{D} , $\mathbf{K}_y^l, \mathbf{K}_x^l, \mathbf{K}_z^l \in \mathbb{R}^{T \times TL}$ are kernel matrices where each row is computed according to one sample l of \mathbf{Z} . Since there is no analytical solution for $\beta_w, \beta_{q,d}$, we update those parameters using gradient descent. The full derivation is deferred to Appendix.

4.2 The auxiliary distributions

The previous steps help approximate the posterior $p(\mathbf{Z} | \cdot)$ by variational posterior $q(\mathbf{Z} | \cdot)$ and estimate the density of $p(\mathbf{Y} | \mathbf{W}, \mathbf{Z}, \mathbf{S})$. To estimate the causal effect, we need three more distributions: $p(\mathbf{Y} | \mathbf{S}, \mathbf{X}, \mathbf{W})$, $p(\mathbf{W} | \mathbf{S}, \mathbf{X})$, $p(\mathbf{S} | \mathbf{X})$. We denote their approximate forms as $\hat{p}(\mathbf{Y} | \mathbf{S}, \mathbf{X}, \mathbf{W})$, $\hat{p}(\mathbf{W} | \mathbf{S}, \mathbf{X})$, $\hat{p}(\mathbf{S} | \mathbf{X})$, respectively, and estimate parameters of those distribution directly using classical representer theorem. Here we briefly describe $\hat{p}(\mathbf{W} | \mathbf{S}, \mathbf{X})$, learning the other distributions are similar and deferred to Appendix. The regularized empirical risk obtained from the log-likelihood of $\hat{p}(\mathbf{W} | \mathbf{S}, \mathbf{X})$ is as follows:

$$\hat{\mathcal{L}}_{\hat{p}_w} = - \sum_{t=1}^T \left[W_t \log \varphi(f_{\hat{p}_w}^t) + (1 - W_t) \log \varphi(-f_{\hat{p}_w}^t) \right] + \Omega_{\hat{p}_w} (\|f_{\hat{p}_w}\|_{\mathcal{H}_{\hat{p}_w}}^2),$$

where $f_{\hat{p}_w}^t = f_{\hat{p}_w}(W_{t-1}, S_t, X_t)$. By classical representer theorem, the minimized form of $f_{\hat{p}_w}$ is: $f_{\hat{p}_w} = \sum_{i=1}^T \beta_i^{\hat{p}_w} \kappa_{\hat{p}_w}(\cdot, [W_{i-1}, S_i, X_i])$ with $\beta_i^{\hat{p}_w}$ to be learned. We note that the above objective function is convex under representer theorem.

5 Experiments

In this section, we examine the performance of our framework on causal inference from temporal data in both synthetic and real-world datasets. We compare with the following baselines: (i) POTS is a potential outcomes-based model for time series data (Bojinov and Shephard, 2019). The key factor of the POTS is the ‘adapted propensity score’. We have implemented two versions of adapted propensity score. The first one uses fully connected neural network. Herein, we assume that $p(W_t | \mathbf{W}_{t-1}, \mathbf{Y}_{t-1}) = p(W_t | W_{t-1}, Y_{t-1}) = \text{Bern}(W_t | f(W_{t-1}, Y_{t-1}))$ with $f(W_{t-1}, Y_{t-1})$ is a neural network taking the observed value of W_{t-1}, Y_{t-1} as input to predict W_t . The second one uses Long-Short Term Memory (LSTM) to estimate $p(W_t = w_t | \mathbf{W}_{t-1}, \mathbf{Y}_{t-1})$. We term these implementations POTS-FC and POTS-LSTM, respectively. (ii) TARNets (also called CFRNet) is a popular framework for inferring treatment effect by Shalit et al. (2017). We have used their code, which is available online (see Table 2 for the link). (iii) CEVAE is a causal inference framework based on variational auto-encoders (Louizos et al., 2017). The code of this method is also available online (see Table 2 for the link). (iv) FCA (fairness through causal awareness by Madras et al. (2019)) is an extension of CEVAE where they consider two types of confounder: observed and latent ones.

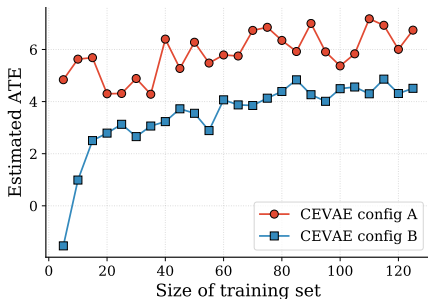


Figure 3: Estimated ATE using CEVAE (Louizos et al., 2017) with different configurations of neural networks. *CEVAE config A*: 6 hidden layers, 100 nodes each layer, *CEVAE config B*: 3 hidden layers, 20 nodes each layer. Both configurations use the same activation function, learning rate, and optimization algorithm. Inconclusive hypothesis may be drawn for a different neural network setup.

5.1 Synthetic experiments

Instability of ATE values inferred using neural networks-based approaches: Figure 3 shows that two different estimated ATE values are produced by using two different configurations of neural networks. The setup is that of (Louizos et al., 2017) where we used different configurations as follows. *CEVAE config A*: 6 hidden layers, 100 nodes each layer, *CEVAE config B*: 3 hidden layers, 20 nodes each layer. Both configurations use the same activation function, learning rate, and optimization algorithm. Hence inconclusive hypothesis may be drawn as a result of using different neural network setups.

Datasets: It is worth noting that obtaining ground truth for evaluating causal inference methods is a challenge. Thus most of the state-of-the-art methods are evaluated with synthetic or semi-synthetic datasets (Louizos et al., 2017). This set of experiments is conducted on 4 synthetic datasets and one benchmark dataset IHDP (Shalit et al., 2017; Louizos et al., 2017). Specifically, we sample data for Z_t, W_t, X_t, S_t, Y_t from their corresponding distributions with length $T = 200$. The ground truth nonlinear functions f_y, f_w, f_z, f_x, f_s with respect to the distributions are fully connected neural networks. Using different numbers of the hidden layers, i.e., 2, 4, and 6, we construct three datasets, namely TD2L, TD4L, and TD6L. For these 3 datasets, we sample the latent confounder variable \mathbf{Z} with Markovian property. We also construct another dataset, TD6L-*iid*, that uses 6 hidden layers but with the *iid* latent confounder variable \mathbf{Z} , i.e., $Z_t \perp\!\!\!\perp Z_s, \forall t, s$. The last dataset, IHDP, is also a dataset assuming *iid* confounder variables. Each dataset has 10 replications. For each replication of a dataset, we use the first 64% for training, the next 20% for validation, and the last 16% for testing. Here we briefly describe construction of the synthetic data, details are presented in Appendix.

Two setups of our method: We examine two setups for our method, one with kernel method to model the nonlinear function and another one with the neural networks. Specifically, we denote (i) **Our Model+RT** as our framework using kernel representer theorem to model the nonlinear functions and (ii) **Our Model+NN j L** ($j \in \{2, 4, 6\}$) as our framework using neural networks to model the nonlinear functions, where j is the number of hidden layers.

The results and discussions: Table 2 reports the mean absolute error (MAE) of average treatment effect (ATE) from our methods and the baselines. The best result as well as the runner-up on each dataset is highlighted using bold. We observe the following results:

- The performance of our model is competitive for the first three datasets. This is owing to the fact that our framework is *suited* for temporal data. This verifies the effectiveness of our proposed framework on the inference of the causal effect, for the temporal data, especially with the latent

Table 2: Mean absolute error (MAE) of the estimated average treatment effect (ATE) on different datasets.

Method	Temporal Data (latent markovian confounders)			IID Data (<i>iid</i> confounders)	
	TD2L	TD4L	TD6L	TD6L-iid	IHDP
Our Method+RT	0.299 ± 0.069	0.193 ± 0.188	0.237 ± 0.056	0.412 ± 0.116	0.290 ± 0.076
Our Method+NN2L	0.369 ± 0.080	0.395 ± 0.162	0.396 ± 0.169	0.390 ± 0.107	4.057 ± 0.109
Our Method+NN4L	0.413 ± 0.092	0.309 ± 0.063	0.313 ± 0.060	0.398 ± 0.104	1.048 ± 0.441
Our Method+NN6L	0.477 ± 0.102	0.325 ± 0.069	0.297 ± 0.070	0.388 ± 0.106	0.306 ± 0.063
POTS-FC	1.477 ± 0.220	1.243 ± 0.219	1.180 ± 0.177	0.470 ± 0.081	0.529 ± 0.183
POTS-LSTM	1.316 ± 0.261	1.117 ± 0.232	1.179 ± 0.323	0.593 ± 0.102	0.613 ± 0.137
TARNets *	0.780 ± 0.131	0.570 ± 0.098	0.701 ± 0.131	0.568 ± 0.091	0.424 ± 0.100
CEVAE **	1.166 ± 0.247	1.428 ± 0.709	0.705 ± 0.179	0.337 ± 0.093	0.232 ± 0.061
FCA	0.391 ± 0.078	1.065 ± 0.504	0.682 ± 0.080	0.393 ± 0.103	0.261 ± 0.063

* We used code from: <https://github.com/clinicalml/cfrnet>

** We used code from: <https://github.com/AMLab-Amsterdam/CEVAE>

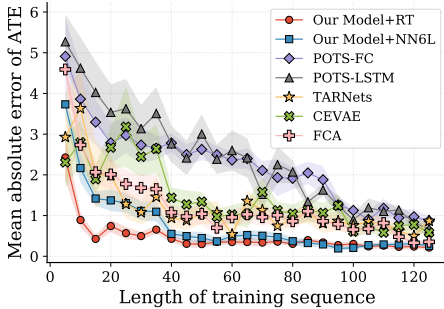


Figure 4: Mean absolute error of the estimated ATE based on different lengths of the training sets.

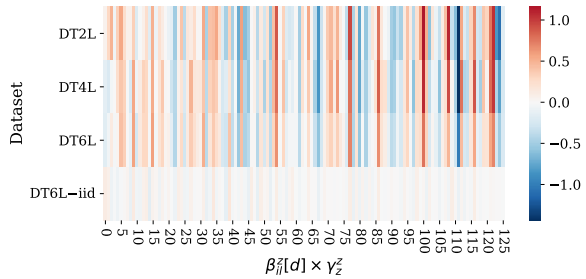


Figure 5: The heatmap of $\beta_{il}^z[d] \times \gamma_z^z$.

Markov confounders.

- For Our Model+RT and Our Model+NNjL, we observe that Our Model+RT generally outperforms Our Model+NNjL, which demonstrates the superiority of kernel method to neural network. This is because using kernel method enables the convexity of the objective, and thus leads to a cheaper and more efficient inference procedure.
- The use of representer theorem returns *similar values* for the ATE. Contrast this to the instability issue, as shown in Figure 3, where *different values* of ATE are being inferred using different configurations of neural network. This highlights one of the advantages of our framework.
- We use *the same architecture and kernels* for all the datasets, showing the flexibility of our kernel method in capturing different kinds of nonlinear functions.
- Our framework with neural networks also outperforms the other baselines (POTS, TARNets, CVAE, FCA), this is because we consider the time-dependency in the latent confounders, while the others do not take into account such property.
- For the last two datasets that use the *iid* data, our methods give comparable results with the other baselines, which are designed for *iid* data. We will further analyze this issue in the following section.

Figure 4 presents the convergence of each method on dataset TD6L, over different lengths of the

training set $T_{\text{train}} \in \{5, 10, \dots, 125\}$. In general, the more training data we have, the smaller the error of the estimated ATE. The figure reveals that our method (blue line) starts to converge from around $T_{\text{train}} = 45$, which is faster than the others. The figure also reveals the estimated ATE of our method is stable with a small error bar.

For the *iid* data (the last two columns of Table 2), our methods achieve comparable results with that of the other baselines. This can be explained as follows. In our setup, $Z_{t,d}$ (the d -th dimension of Z_t) has the following form: $Z_{t,d} = C + \sum_{i=1}^T \sum_{l=1}^L \beta_{il}^z[d] \gamma_z^z k_z(Z_{t-1}, Z_i^l) + \epsilon_t$, where C is a learned bias and ϵ_t is the white noise. Figure 5 presents the heatmap of $\beta_{il}^z[d] \times \gamma_z^z$ (with $i = 1, \dots, T$; $l = 1$; $d = 1$) learned from our inference algorithm. The last row in Figure 5 shows that when learning from the data with *iid* confounders, the learned weights is around 0 (white color), which breaks the connection from Z_t to Z_{t-1} , thus makes these two variables independent to each other.

5.2 Real data: gold–oil dataset

Gold is one of the most transactable precious metals, and oil is one of the most transactable commodities. Rising oil price generates higher inflation which strengthens the demand for gold and hence pushes up the gold price, (Le and Chang, 2011; Šimáková, 2011). In this section, we examine our model performance in estimating the causal relationships of the prices between crude oil and gold. In particular, we aim to quantify the causal effects from the price of crude oil to that of gold. The dataset in this experiment consists of monthly prices of some commodities including gold, crude oil, beef, chicken, cocoa-beans, rice, shrimp, silver, sugar, gasoline, heating oil and natural-gas from May 1989 to May 2019. We consider the price of gold as the outcome \mathbf{Y} , and the trend of crude oil’s price as the treatment \mathbf{W} . Specifically, we cast an increase of crude oil’s price as 1 ($W_t = 1$) and a decrease of crude oil’s price as 0 ($W_t = 0$). Denote the prices of gasoline, heating oil, natural-gas, beef, chicken, cocoa-beans, rice, shrimp, silver and sugar as proxy variables \mathbf{X} . The aim is to estimate the causal effects of \mathbf{W} to \mathbf{Y} given \mathbf{X} .

In our setup, W_t only represents *increase* or *decrease* of crude oil’s price, neglecting the constant case. To evaluate the causal effects of an increasing oil price and a constant one, we evaluate the effect path and ATE between two sequences of treatments $\mathbf{W}_1 = [1, 1, 1, 1, \dots, 1, 1]^\top$ (increasing crude oil prices) and $\mathbf{W}_2 = [0, 1, 0, 1, \dots, 0, 1]^\top$ (alternating decreasing and increasing crude oil prices, and constant on average). Figure 6 (a) and (b) present the effect paths and ATE of the increasing crude oil price over a constant one. The ATE computed from our framework gives a value of 4.8. In other words, given a period when the price of crude oil increases, the average gold price in this period is about to increase 4.8. This increase is equivalent to an increase of 0.77% in the gold price over the period ($4.8 / \{T^{-1} \sum_{t=1}^T Y_t^{obs}\} = 0.77\%$). To validate the 0.77% increase in gold price, we contrast and compare this with the results reported in Šimáková (2011) that show the “percentage increase in oil price leads to a 0.64% increase in gold price”. We note that our results give similar order of magnitude and the slight difference may be attributed to our observations that are based on data from May 1989 to May 2019, whilst the analysis in Šimáková (2011) are based on the data from 1970 to 2010.

In Figure 7, we further performed another experiment with $\mathbf{W}_1 = [1, 0, \dots, 1, 0]^\top$ and $\mathbf{W}_2 = [0, 1, \dots, 0, 1]^\top$. In this case, both treatment paths represent the alternating variation of crude oil prices. Specifically, the former increases first and then decreases, while the latter is on the opposite.

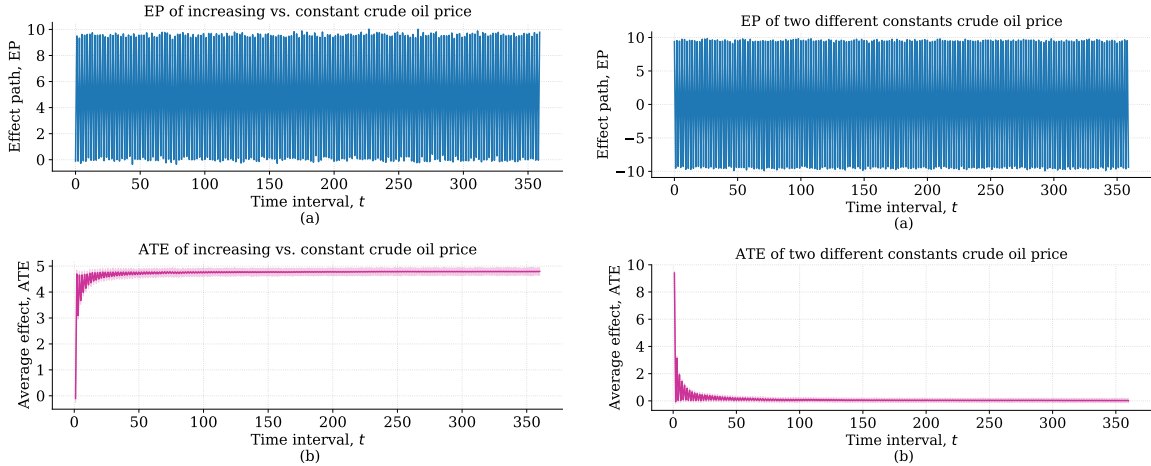


Figure 6: (a) The estimated EP and (b) ATE between two treatment paths $[1, 1, 1, 1, \dots, 1, 1]^\top$ and $[0, 1, 0, 1, \dots, 0, 1]$.

Figure 7: (a) The estimated EP and (b) ATE between two treatment paths $[1, 0, 1, 0, \dots, 1, 0]^\top$ and $[0, 1, 0, 1, \dots, 0, 1]$.

The average treatment effect is expected to be around 0. From Figure 7, the ATE derived from our method is 0.0045, which is in line with the expectation. To check on statistical significance, we performed a one group t -test on the effect path (EP) (Definition 1), and the population mean to be tested is 0. The p -value given by the t -test is 0.9931, which strongly accepts the null hypothesis that the average treatment effect equals to 0. This again verifies the effectiveness of our method.

6 Conclusion

We have developed a causal modeling framework that admits confounders as random processes, generalizing recent work where the confounders are assumed to be independent and identically distributed. Exploiting the Markovian property, we study the causal effects over time using variational inference in conjunction with an alternative form of the Representer Theorem with a random input space.

Our algorithm supports causal inference from the observed outcomes, treatments, and covariates, without any parametric specification of the components and their relations. This property is important for capturing real-life causal effects in SCM, where non-linear functions are typically placed in the priors. Our setup admits non-linear functions modulating the SCM with estimated parameters that turn out to have *closed-form* solutions. This approach compares favorably to state-of-the-art techniques that model similar non-linear functions to estimate the causal effects with neural networks, which usually involve extensive model tuning and architecture building.

We have empirically demonstrated the promise of our framework. The next step is to derive generalization bounds on the stochastic causal confounders. We will also examine how the framework can be applied in different real-life domains.

References

- Bahadori, M. T. and Liu, Y. (2012). On causality inference in time series. In *2012 AAAI Fall Symposium Series*.
- Bojinov, I. and Shephard, N. (2019). Time series experiments and causal estimands: exact randomization tests and trading. *Journal of the American Statistical Association*, pages 1–36.
- Eichler, M. (2005). A graphical approach for evaluating effective connectivity in neural systems. *Philosophical Transactions of the Royal Society B: Biological Sciences*, 360(1457):953–967.
- Eichler, M. (2007). Granger causality and path diagrams for multivariate time series. *Journal of Econometrics*, 137(2):334–353.
- Eichler, M. (2009). Causal inference from multivariate time series: What can be learned from granger causality. In *13th International Congress on Logic, Methodology and Philosophy of Science*.
- Eichler, M. and Didelez, V. (2010). On granger causality and the effect of interventions in time series. *Lifetime data analysis*, 16(1):3–32.
- Frees, E. W. et al. (2004). *Longitudinal and panel data: analysis and applications in the social sciences*. Cambridge University Press.
- Granger, C. W. (1980). Testing for causality: a personal viewpoint. *J. Economic Dynamics and control*, 2:329–352.
- Guo, R., Cheng, L., Li, J., Hahn, P. R., and Liu, H. (2018). A survey of learning causality with data: Problems and methods. *arXiv preprint arXiv:1809.09337*.
- Horvitz, D. G. and Thompson, D. J. (1952). A generalization of sampling without replacement from a finite universe. *Journal of the American statistical Association*, 47(260):663–685.
- Huang, B., Zhang, K., Gong, M., and Glymour, C. (2019). Causal discovery and forecasting in nonstationary environments with state-space models. In *Proceedings of the 36th International Conference on Machine Learning*.
- Kamiński, M., Ding, M., Truccolo, W. A., and Bressler, S. L. (2001). Evaluating causal relations in neural systems: Granger causality, directed transfer function and statistical assessment of significance. *Biological cybernetics*, 85(2):145–157.
- Kimeldorf, G. S. and Wahba, G. (1970). A correspondence between bayesian estimation on stochastic processes and smoothing by splines. *The Annals of Mathematical Statistics*, 41(2):495–502.
- Le, T.-H. and Chang, Y. (2011). Oil and gold: correlation or causation? Technical report, Nanyang Technological University, School of Social Sciences, Economic Growth Centre.
- Louizos, C., Shalit, U., Mooij, J. M., Sontag, D., Zemel, R., and Welling, M. (2017). Causal effect inference with deep latent-variable models. In *Advances in Neural Information Processing Systems*, pages 6446–6456.
- Madras, D., Creager, E., Pitassi, T., and Zemel, R. (2019). Fairness through causal awareness: Learning causal latent-variable models for biased data. In *Proceedings of the Conference on Fairness, Accountability, and Transparency*, pages 349–358. ACM.

- Montgomery, M. R., Gragnolati, M., Burke, K. A., and Paredes, E. (2000). Measuring living standards with proxy variables. *Demography*, 37(2):155–174.
- Ning, B., Ghosal, S., Thomas, J., et al. (2019). Bayesian method for causal inference in spatially-correlated multivariate time series. *Bayesian Analysis*, 14(1):1–28.
- Osama, M., Zachariah, D., and Schön, T. (2019). Inferring heterogeneous causal effects in presence of spatial confounding. In *Proceedings of the 36th International Conference on Machine Learning*.
- Pearl, J. (2000). *Causality: models, reasoning and inference*, volume 29. Springer.
- Pearl, J. (2009). Causal inference in statistics: An overview. *Statistics surveys*, 3:96–146.
- Pearl, J. (2010). Causal inference. In *Causality: Objectives and Assessment*, pages 39–58.
- Peters, J., Janzing, D., and Schölkopf, B. (2013). Causal inference on time series using restricted structural equation models. In *Advances in Neural Information Processing Systems*, pages 154–162.
- Rakesh, V., Guo, R., Moraffah, R., Agarwal, N., and Liu, H. (2018). Linked causal variational autoencoder for inferring paired spillover effects. In *Proceedings of the 27th ACM International Conference on Information and Knowledge Management*, pages 1679–1682. ACM.
- Riegg, S. K. (2008). Causal inference and omitted variable bias in financial aid research: Assessing solutions. *The Review of Higher Education*, 31(3):329–354.
- Rubin, D. B. (2005). Causal inference using potential outcomes: Design, modeling, decisions. *Journal of the American Statistical Association*, 100(469):322–331.
- Schölkopf, B., Herbrich, R., and Smola, A. J. (2001). A generalized representer theorem. In *International conference on computational learning theory*, pages 416–426. Springer.
- Shalit, U., Johansson, F. D., and Sontag, D. (2017). Estimating individual treatment effect: generalization bounds and algorithms. In *Proceedings of the 34th International Conference on Machine Learning*, pages 3076–3085.
- Šimáková, J. (2011). Analysis of the relationship between oil and gold prices. *Journal of finance*, 51(1):651–662.